

UCSF

UC San Francisco Previously Published Works

Title

Targeting the mutant PIK3CA gene by DNA-alkylating pyrrole-imidazole polyamide in cervical cancer

Permalink

<https://escholarship.org/uc/item/5kd9m2xw>

Journal

Cancer Science, 112(3)

ISSN

1347-9032

Authors

Krishnamurthy, Sakthisri
Yoda, Hiroyuki
Hiraoka, Kiriko
et al.

Publication Date

2021-03-01





DOI

10.1111/cas.14785

Peer reviewed

ORIGINAL ARTICLE

Targeting the mutant *PIK3CA* gene by DNA-alkylating pyrrole-imidazole polyamide in cervical cancer

Sakthisri Krishnamurthy^{1,2,3} | Hiroyuki Yoda²  | Kiriko Hiraoka¹ | Takahiro Inoue¹ | Jason Lin¹  | Yoshinao Shinozaki¹ | Takayoshi Watanabe² | Nobuko Koshikawa¹ | Atsushi Takatori²  | Hiroki Nagase¹ 

¹Division of Cancer Genetics, Chiba Cancer Center Research Institute, Chiba, Japan

²Division of Innovative Cancer Therapeutics, Chiba Cancer Center Research Institute, Chiba, Japan

³Graduate School of Medical and Pharmaceutical Sciences, Chiba University, Chiba, Japan

Correspondence

Atsushi Takatori, Division of Innovative Cancer Therapeutics, Chiba Cancer Center Research Institute, 666-2 Nitona-cho, Chuo-ku, Chiba 260-8717, Japan.
Email: atakatori@chiba-cc.jp

Hiroki Nagase, Division of Cancer Genetics, Chiba Cancer Center Research Institute, 666-2 Nitona-cho, Chuo-ku, Chiba 260-8717, Japan.
Email: hnagase@chiba-cc.jp

Funding information

Ministry of Education, Culture, Sports, Science and Technology, Grant/Award Number: JP25830092; Japan Society for the Promotion of Science, Grant/Award Number: JP16H01579, JP17H03602 and JP26290060; Princess Takamatsu Cancer Research Fund; Takeda Science Foundation

Abstract

PIK3CA is the most frequently mutated oncogene in cervical cancer, and somatic mutations in the *PIK3CA* gene result in increased activity of PI3K. In cervical cancer, the E545K mutation in *PIK3CA* leads to elevated cell proliferation and reduced apoptosis. In the present study, we designed and synthesized a novel pyrrole-imidazole polyamide-*seco*-CBI conjugate, P3AE5K, to target the *PIK3CA* gene bearing the E545K mutation, rendered possible by nuclear access and the unique sequence specificity of pyrrole-imidazole polyamides. P3AE5K interacted with double-stranded DNA of the coding region containing the E545K mutation. When compared with conventional PI3K inhibitors, P3AE5K demonstrated strong cytotoxicity in E545K-positive cervical cancer cells at lower concentrations. *PIK3CA* mutant cells exposed to P3AE5K exhibited reduced expression levels of *PIK3CA* mRNA and protein, and subsequent apoptotic cell death. Moreover, P3AE5K significantly decreased the tumor growth in mouse xenograft models derived from *PIK3CA* mutant cells. Overall, the present data strongly suggest that the alkylating pyrrole-imidazole polyamide P3AE5K should be a promising new drug candidate targeting a constitutively activating mutation of *PIK3CA* in cervical cancer.

KEYWORDS

cervical cancer, E545K mutation, PI3K inhibitor, *PIK3CA* gene, pyrrole-imidazole polyamide-*seco*-CBI

1 | INTRODUCTION

Cervical cancer as a “mother killer” is one of the most common cancers in females, especially in the developing world where human papillomavirus (HPV) vaccination is not available. In 2012, 266 000 cases of cervical cancer-induced death were reported worldwide, with an expected increase to 410 000 by 2030.¹ Although patients diagnosed with early stage cervical cancer are

curable with current standard therapy, advanced or recurrent cases have poor prognosis.^{2,3} In cases of metastatic or recurrent cervical cancers, it is thought that the PI3K/AKT/mTOR pathway is highly dysregulated,⁴ in which *PIK3CA*, a gene encoding the p110 alpha catalytic subunit of Class I PI3K, can become amplified in copy number and activated by certain driving mutations. With its status as the second most commonly mutated gene in human endometrial cancer,^{5,6} activating mutations in *PIK3CA* are associated

This is an open access article under the terms of the Creative Commons Attribution-NonCommercial License, which permits use, distribution and reproduction in any medium, provided the original work is properly cited and is not used for commercial purposes.

© 2020 The Authors. *Cancer Science* published by John Wiley & Sons Australia, Ltd on behalf of Japanese Cancer Association.

with cancer cell survival, invasion, metastasis, angiogenesis, and anti-apoptosis.^{4,7,8} Among those mutations of *PIK3CA*, the E545K mutation is a major hotspot mutation, occurring in 23–36% of cervical cancer cases.^{8,9}

Some PI3K inhibitors have been developed and are under clinical investigation for use in cancer treatments, such as BYL719 (PI3K α -isoform specific inhibitor), and dozens of other new inhibitors are in clinical trial¹⁰; however, the clinical studies of some inhibitors have been discontinued due to their high toxicities.^{11,12} There have been some conflicting breast cancer clinical trials that suggested that long-term treatment of PI3K inhibitors may induce drug resistance and subsequently partial regression.^{13–15} Although some PI3K inhibitors have been shown to sensitize cervical cancer cells to chemotherapy,¹⁶ the E545K mutation is associated with cisplatin resistance and shorter survival in advanced cervical cancer.¹⁷

Pyrrole-imidazole (PI) polyamides are programmable DNA minor-groove binders with high sequence specificity.¹⁸ DNA sequence recognition depends on the combination of pyrrole and imidazole in its primary configuration, with a strong preference for C/G binding by pyrrole/imidazole pairings. After further functionalization of PI polyamides with alkylating agents such as *seco*-CBI, the resultant conjugate can form a DNA adduct by covalently joining the polyamide at the N3 adenine of its specific recognition motif.¹⁹ PI polyamides can modulate gene expression by minor-groove binding at specific sites, altering the local DNA architecture and thereby disturbing RNA transcription in progress, all of which eventually lead to decreased expression levels of the targeted genes.²⁰ To date, various reports have shown that PI polyamides are capable of downregulating the expression of specific genes,^{21–24} with a notable example showing antitumor activity against colon cancer cell lines harboring *KRAS* G12D/V mutations.²¹

Utilizing this gene-level approach, we here propose the use of a new promising alkylating PI polyamide, P3AE5K, to target the E545K mutation in *PIK3CA*. P3AE5K showed high sequence-specific binding affinity to its target nucleotide sequence, and downregulated mutant *PIK3CA* expression in cervical cancer cells. This polyamide candidate also induced significant apoptosis in *PIK3CA* mutant cervical cancer cells, and reduced tumor growth in a mouse xenograft tumor model.

2 | MATERIALS AND METHODS

2.1 | Reagents

Solvents and reagents used for the synthesis were as follows: Fmoc-Pyrrole oxime resin, *N*-methyl-2-pyrrolidone (NMP), *N,N*-diisopropylethylamine (DIEA), Fmoc-Pyrrole-COOH, Fmoc-Imidazole-COOH, Fmoc-Pyrrole-Imidazole-COOH, Fmoc- β -COOH and Fmoc- γ -COOH (Wako Chemicals, Tokyo, Japan); PyBOP and Fmoc- β -alanine (Novabiochem, Tokyo, Japan); high-performance liquid chromatography (HPLC) grade acetonitrile piperidine and acetic anhydride (SIGMA); and HCTU (Peptide Institute). LY294002

and BYL719 were purchased from Wako Chemicals and Selleck, respectively.

2.2 | Synthesis of polyamide

We applied a solid phase method as a stepwise reaction using a semi-automated PSSM-8 peptide synthesizer (Shimadzu) in a 10 μ mol scale.^{25–27} The alkylating agent, indole-*seco*-CBI, was prepared following previously reported procedures.²⁸ The HPLC LC-20 system (Shimadzu) was used to purify the PI polyamides through a 10 \times 150 mm Phenomenex Gemini-NX3u 5-ODS-H reverse-phase column (Phenomenex) with 0.1% acetic acid in Millipore Milli-Q[®] water and acetonitrile with a flow rate of 10 ml/min. The purified P3AE5K backbone was dissolved in NMP, followed by addition of 20% DIEA, and 3.5 eq PyBOP and then incubated for 20 min at room temperature. The conversion of P3AE5K-COOH to the activated 1-hydroxybenzotriazole ester was verified by analytical HPLC. Conjugation of NH₂-indole-*seco*-CBI proceeded at 3.5 eq at room temperature for 24 h under agitation at 1200 rpm. The conjugate was purified by HPLC (30–75% binary gradient, using 0.1% acetic acid in Millipore Milli-Q water and acetonitrile, with a 340 nm peak observed at 17.6–18.4 min). The purified product was concentrated and lyophilized for storage, and reconstituted in dimethyl sulfoxide (DMSO) for use in further experiments. Electrospray ionization mass spectrometry (ESI-MS) characterization: $[M+H]^+m/z$ calcd for C₈₉H₉₂ClN₃₁O₁₆ = 1886.70, found 1886.50 (Figure S1). The log P values were estimated by using reverse-phase HPLC, as previously described.²⁹ Retention times of compounds were measured using a Prominence HPLC system (Shimadzu Industry) and a 150 \times 4.6 mm Gemini-NX C18 110Å reverse-phase column (Phenomenex) under isocratic conditions (0.1% acetic acid : acetonitrile = 57 : 43) at a flow rate of 1 mL/min. A standard curve was constructed plotting the log P values vs retention times (t) of reference compounds retrieved from PubChem (<https://pubchem.ncbi.nlm.nih.gov/>), such as curcumin (t = 11.92, log P = 3.29), indole (t = 5.29, log P = 2.14) and 4-chloroaniline (t = 3.95, log P = 1.83), and then the log P value of P3AE5K was estimated from the retention time (t = 11.71).

2.3 | Surface plasmon resonance (SPR) assay

Surface plasmon resonance assays were performed to analyze the binding affinity of P3AE5K using the Biacore X100 system, in accordance with a previous study.²⁶ P3AE5K was coupled with dimethylaminopropylamine (Dp), and the resultant P3AE5K-Dp was used in analyses. Two biotinylated hairpin oligonucleotides corresponding to the E545K-mutant PI3K (full match) sequence (MUT-B1, AAG) and the wild-type PI3K sequence (WT-B1, GAG) (Figure S1) were immobilized on a streptavidin-coated sensor chip. HBS-EP buffer (10 mmol/L HEPES pH 7.4, 150 mmol/L NaCl, 3 mmol/L EDTA, and 0.005% Surfactant P20) with 0.4% DMSO at 25°C was used. Samples were injected at a flow rate of 30 μ l/min.

Biacore X100 Evaluation Software version 2.0 was used to calculate the dissociation rate constant (K_d). The binding model with mass transfer was used to fit all of the sensorgrams to give 2 state reactions.

2.4 | Cell culture

ME-180 and CaSki cells, both heterozygous *PIK3CA* mutant (E545K) cervical cancer cell lines, were obtained from the RIKEN BioResource Center and cultured in RPMI-1640 medium (Sigma). The SiHa cell line (wild-type *PIK3CA*) was purchased from the American Type Culture Collection (ATCC) and cultured in modified Eagle's medium (MEM) (Sigma). All cell cultures were supplemented with 10% heat-inactivated FBS and 1% antibiotics (streptomycin and penicillin). The cell lines were maintained at 37°C in 5% CO₂ in air. All cells were authenticated by the suppliers and used within 10 passages after thawing. The lines were tested for *Mycoplasma* contamination was tested using a *Mycoplasma* Detection Set (TaKaRa).

2.5 | Cell viability assay

Cell viability was assessed by water soluble tetrazolium salts (WST) assay with Cell Counting Kit-8 (Dojindo). Cells were seeded in triplicate in 96-well plates at a concentration of 3000 cells per well and allowed to adhere for 16-24 h. Cells were treated with increasing concentrations of P3AE5K or PI3K inhibitors, and 0.2% of DMSO was used as a control. After 48 h, 10 µl of WST-8 reagent was added to each well and cells were incubated for 1 h. The absorbance was measured at 450 nm on a microplate reader (MTP-310, Corona, Ibaraki, Japan).

2.6 | Quantitative and real-time PCR

Cells were seeded at a concentration of 1×10^5 cells/well in a 6-well plate and allowed to attach overnight. The cells were then treated with 10 nmol/L of P3AE5K or 0.2% of DMSO as a control. After 24 h of treatment, the cells were lysed and RNA was extracted using the RNeasy Plus Mini kit (Qiagen) in accordance with the manufacturer's protocol. For reverse transcription, cDNA was obtained from 500 ng purified RNA using the Superscript VILO master mix (Invitrogen). *PIK3CA* and *RPS18* mRNA expression levels were measured using the SYBR green real-time system and the following primers: *PIK3CA* Forward, 5'-TACCTTGTTCCAATCCCAGG-3' and *PIK3CA* Reverse, 5'-CTTTCGGCCTTAACAGAGC-3'; *RPS18* Forward, 5'-GAGGATGAGGTGGAACGTGT-3' and *RPS18* Reverse, 5'-TCTTCAGTCGCTCCAGGTCT-3'. PCR reactions were performed on an ABI 7500 Real-Time PCR system (Applied Biosystems), and *RPS18* was used as an internal control. All experiments were performed in triplicate.

2.7 | Immunoblot

P3AE5K-treated cells were lysed using RIPA buffer supplemented with phosphatase and complete proteinase inhibitor. Protein concentration was measured by BCA protein assay kit (Thermo). Equal amounts of proteins were separated by SDS-PAGE and then transferred to PVDF membranes. The membranes were blocked with 5% skimmed milk and subjected to immunoblotting using the following primary antibodies: anti-p110alpha (Cell Signaling Technology), anti-phospho-PI3 kinase p85 (Cell Signaling Technology), anti-phospho Akt (Ser473) (Cell Signaling Technology), anti-Akt (Cell Signaling Technology), anti-phospho-p70 S6 kinase (Cell Signaling Technology), anti-p70 S6 kinase (Cell Signaling Technology), anti-actin (Santa Cruz Biotechnology), anti-PARP (Cell Signaling Technology), anti-Bax (Cell Signaling Technology), anti-phospho-H2AX (BioLegend, San Diego, CA, USA), anti-caspase 9 (Cell Signaling Technology), anti-cleaved caspase 3 (Cell Signaling Technology), anti-Bax (Cell Signaling Technology), and anti-Bcl-2 (Cell Signaling Technology). After incubation with HRP-conjugated secondary antibodies (Cell Signaling Technology), the protein bands were visualized using a chemiluminescence reagent (Thermo). The results were quantified using ImageJ software and fold change relative to DMSO was calculated.

2.8 | Annexin V staining

Apoptosis was detected using the MEBCYTO Annexin V-FITC Kit (MBL). After treatment with DMSO or P3AE5K at different concentrations (10-50 nmol/L) for 48 h, cells were harvested by centrifugation and resuspended in binding buffer. Staining with Annexin V and propidium iodide was performed in accordance with the manufacturer's instructions. Apoptosis rates were measured by flow cytometry (FACSCalibur; BD) using a single laser emitting excitation light at 488 nm. Data were analyzed using FlowJo version 10.6.0 software (BD).

2.9 | Animal tumor models

We received prior approval for in vivo xenograft experiments from the animal care and ethics committee of Chiba Cancer Center Research Institute. Female BALB/c nude mice were obtained from Charles River Laboratories, Yokohama, Japan. For the xenograft experiment, mice (4-6 wk old) were subcutaneously injected with CaSki cervical cancer cells (3×10^6 cells). After tumor size reached 50-70 mm³, the mice were intraperitoneally injected with DMSO or P3AE5K (3 mg/kg/wk) once a wk for 4 wk ($n = 6$ in each group). Tumor size was measured using a caliper and calculated from the formula $V = L \times W \times H \times \pi/6$. The mice were sacrificed at 28 d after first treatment or after the tumor size reached 2000 mm³, and the tumor tissues were resected, fixed in 4% paraformaldehyde, dehydrated with a graded ethanol series and embedded in paraffin. Sections (4 µm) were deparaffinized by immersing in xylene and rehydrated,

followed by staining with H&E in accordance with standard procedures. The sections were subjected to immunohistochemistry using anti-p110 α and anti-phospho Akt (Ser473) antibodies (Cell Signaling Technology).

2.10 | Statistical analysis

Statistical analyses were performed using GraphPad Prism v.6.0 software. Data were represented as mean \pm SD from 3 independent experiments. For in vitro studies, unpaired *t* test was used for the difference between 2 groups and one-way ANOVA followed by Holm-Sidak multiple comparison test for multiple group analysis. For in vivo studies, repeated measures ANOVA followed by Bonferroni post test was used to evaluate the difference in tumor volume between the groups. *P*-values less than .05 were considered statistically significant.

3 | RESULTS

3.1 | Design and synthesis of P3AE5K and its binding affinity

To target the E545K-mutated *PIK3CA* gene, we designed and synthesized a DNA-alkylating PI polyamide, P3AE5K, which binds to the sequence 5'-TWWGCWGGW-3' in *PIK3CA* (where W indicates A or

T; Figure 1A,B); this particular motif led to the chemical configuration of a linear polyamide chain PyPyImPy- β -ImIm- γ -PyPy- β -ImPy (Py = pyrrole; Im = imidazole; β = β -alanine) coupled with *seco*-CBI to obtain P3AE5K. The binding affinity of P3AE5K was examined by SPR assays (Figure S2) using a non-alkylating variant P3AE5K-Dp. We observed its preferential binding to the target mutant oligonucleotide compared with to the mismatched oligonucleotide (wild-type sequence) (Figure 1C). The K_D constants for P3AE5K-Dp for the target and mismatch oligonucleotides were 6.67×10^{-7} and 3.78×10^{-5} M, respectively (Table 1). The binding affinity of P3AE5K to the mutant sequence was 56.7-fold higher than that of the wild-type sequence.

3.2 | Attenuation of *PIK3CA* E545K mutant gene expression by P3AE5K

To analyze the ability of P3AE5K to suppress *PIK3CA* gene expression, human cervical cancer cells with the *PIK3CA* E545K mutation (ME-180 and CaSki cells) and cells without the mutation (SiHa cells) were treated with vehicle or P3AE5K for 24 h, followed by quantitative PCR and western blot analyses. *PIK3CA* mRNA and protein expression levels were markedly suppressed by P3AE5K treatment in ME-180 and CaSki cells, although no effects were observed in P3AE5K-treated SiHa cells (Figure 2). The downregulation of *PIK3CA* was accompanied with marked decrease in the phosphorylation of PI3K downstream molecules, including p85, Akt, and p70 S6 kinase.

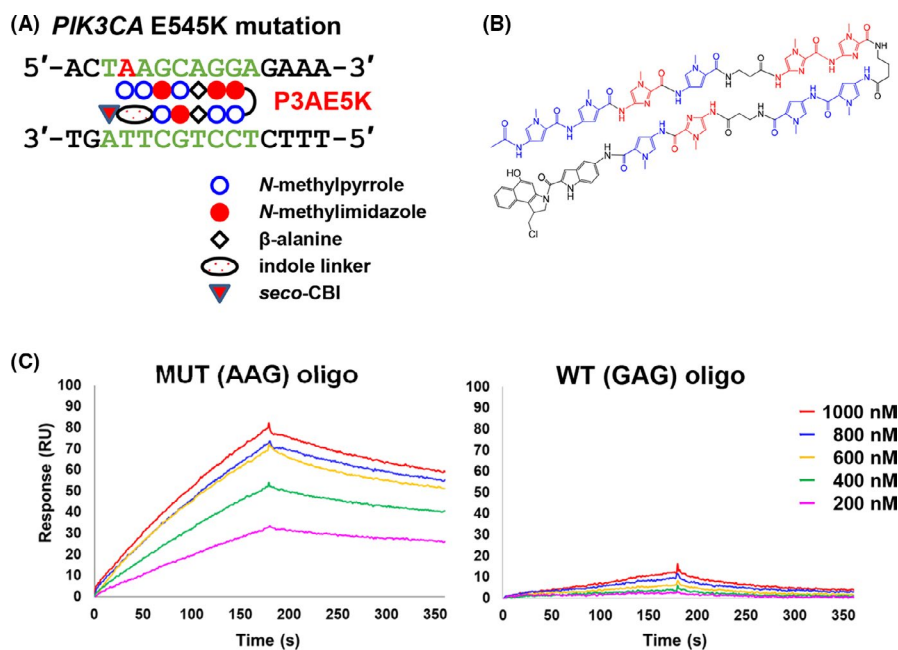


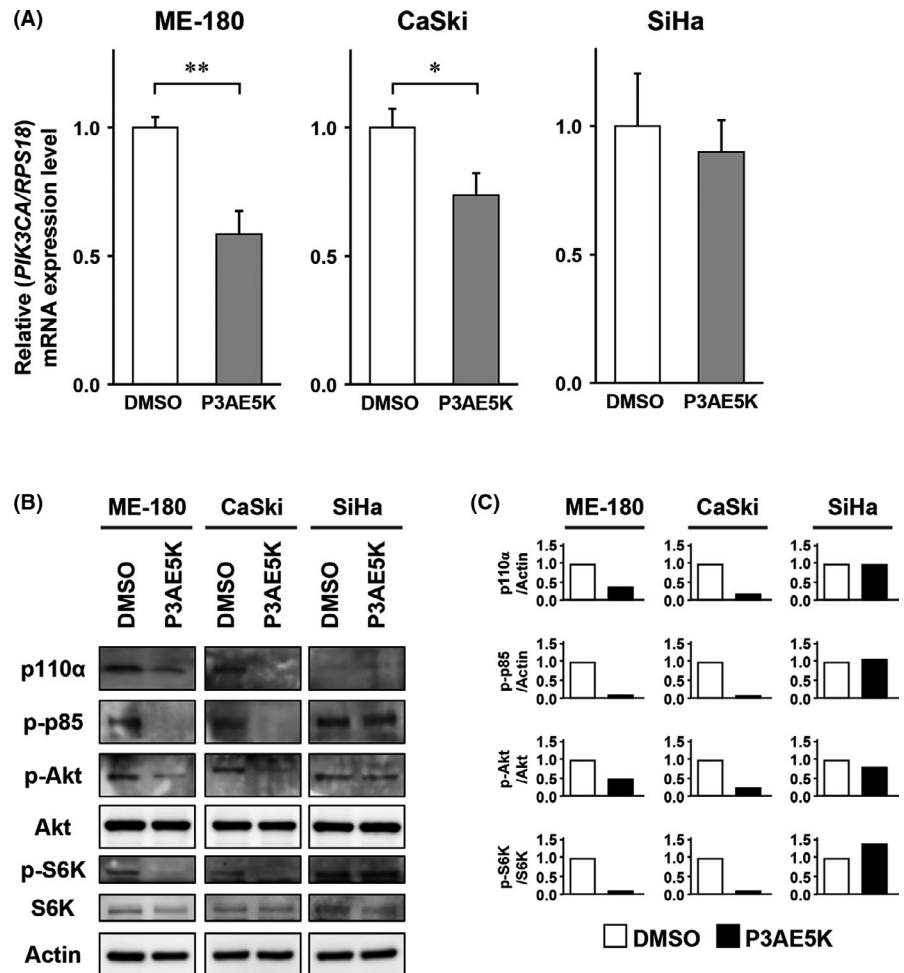
FIGURE 1 Chemical structure and binding affinity of P3AE5K. A, Diagram representation of binding of the hairpin polyamide, P3AE5K, with the 9-bp recognition sequence (green) in exon 9 of the E545K-mutated *PIK3CA* gene (1633G>A in red) at +1633-1641 bp. B, Chemical structure of P3AE5K targeting the *PIK3CA* gene mutation. P3AE5K is a PI polyamide coupled with indole CBI to form the PI *seco*-CBI conjugate. C, SPR sensorgrams for the interaction of P3AE5K-Dp with hairpin DNAs containing the *PIK3CA* E545K mutant sequence or wild-type sequence immobilized on the surface of the sensor chip. The 5 curves of the lowest, mid low, middle, mid high and highest indicate P3AE5K-Dp concentrations of 200, 400, 600, 800 and 1000 nmol/L, respectively

TABLE 1 Evaluation of binding affinity of P3AE5K by SPR assay

PI polyamide	Oligo sequence	K_D (M)	K_A (1/M)	K_d (1/s)	K_a (1/Ms)	Specificity
P3AE5K-Dp	WT-B1 (GAG)	3.78×10^{-5}	2.65×10^{-4}	6.98×10^{-3}	1.85×10^2	–
	MUT-B1 (AAG)	6.67×10^{-7}	1.49×10^{-6}	1.54×10^{-3}	2.31×10^3	56.7

Abbreviations: K_D , dissociation equilibrium constant; K_A , association equilibrium constant; K_a , association rate constant; K_d , dissociation rate constant. K_D was calculated by the following method, $K_D = K_d/K_a$

FIGURE 2 Suppression of PIK3CA expression by P3AE5K. A, Real-time PCR of the relative expression of the *PIK3CA* gene in cervical cancer cells treated with P3AE5K (10 nmol/L) for 24 h. Data were represented as mean \pm SD from 3 independent experiments. *P*-values were determined by unpaired *t* test using GraphPad Prism software ($*P < .05$, $**P < .01$). B, Western blot for the expression of PIK3CA (p110 α) and phosphorylated forms of PI3 kinase p85 (p-p85), Akt (p-Akt) and p70 S6 kinase (p-S6K) in cells treated with P3AE5K (10 nmol/L) for 48 h. Total expression of Akt, p70 S6 kinase or actin was used as an internal control. C, Protein signal intensity was quantified by ImageJ software and the fold change relative to DMSO was represented graphically. Data are the average of 2 independent experiments



3.3 | Impaired cell survival in P3AE5K-treated cervical cancer cells

We next performed WST assays to study changes in cell viability after treatment of P3AE5K and PI3K inhibitors in cervical cancer cells. P3AE5K treatment for 48 h strongly reduced cell viability in ME-180 and CaSki cells, but not in SiHa cells (Figure 3A). The IC_{50} values of P3AE5K were lower than 0.05 μ mol/L in *PIK3CA*-mutated ME-180 and CaSki cells, although *PIK3CA* wild-type SiHa cells showed an IC_{50} of 0.145 μ mol/L (Figure 3B–D). In contrast, the PI3K inhibitors, LY294002 and BYL719, showed similar IC_{50} values in all 3 cell lines, except for BYL719-treated ME-180 cells, which had a relatively low IC_{50} compared with BYL719-treated CaSki cells. These data suggested that P3AE5K possessed higher cytotoxicity comparable with conventional PI3K inhibitors, but

that the *PIK3CA* E545K-mutant cervical cancer cells were preferentially sensitive to P3AE5K.

3.4 | P3AE5K-induced apoptosis in *PIK3CA* mutant cervical cancer cell lines

To examine the effects of P3AE5K on cell death of cervical cancer cells, we performed propidium iodide/Annexin V staining. P3AE5K-treated ME-180 and CaSki cells showed a significant increase in the late apoptotic cell populations compared with vehicle-treated cells, whereas P3AE5K treatment at the same concentration did not induce apoptosis in SiHa cells (Figures 4A and S3). P3AE5K treatment induced apoptosis in ME-180 cells dose dependently, and an increased number of apoptotic cells was observed at 50 nmol/L in CaSki cells (Figure 4B). We further confirmed the pro-apoptotic

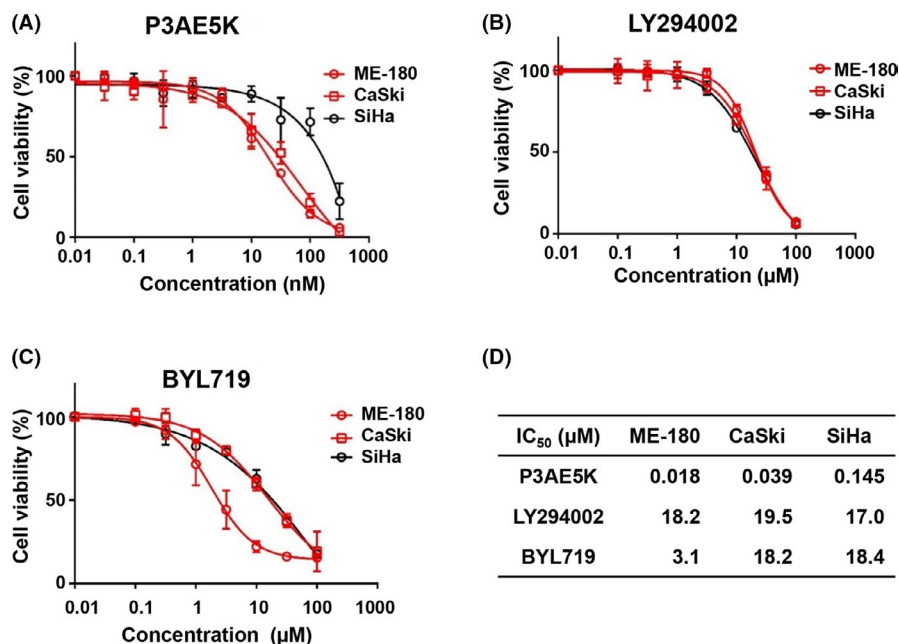


FIGURE 3 Comparison of cell viability of P3AE5K with PI3K inhibitors. Cervical cancer cells were treated with increasing concentrations of P3AE5K (A) or the PI3K inhibitors, LY294002 (B) or BYL719 (C) for 48 h, and cell viability was determined by WST assays. (D) IC₅₀ values of P3AE5K, LY294002, and BYL719

effect of P3AE5K by immunoblotting for markers of apoptosis and DNA damage. P3AE5K treatment displayed the elevated levels of apoptotic markers, including cleavage of PARP, caspase 3 and Bax and downregulation of caspase 9 and Bcl-2 in ME-180 and CaSki cells (Figure 4C,D). Phosphorylated H2AX was also upregulated in P3AE5K-treated ME-180 and CaSki cells, suggesting that a low concentration of P3AE5K was sufficient to induce DNA damage in *PIK3CA*-mutant cervical cancer cells. In contrast, *PIK3CA* wild-type SiHa cells showed no changes in the levels of these markers after P3AE5K treatment.

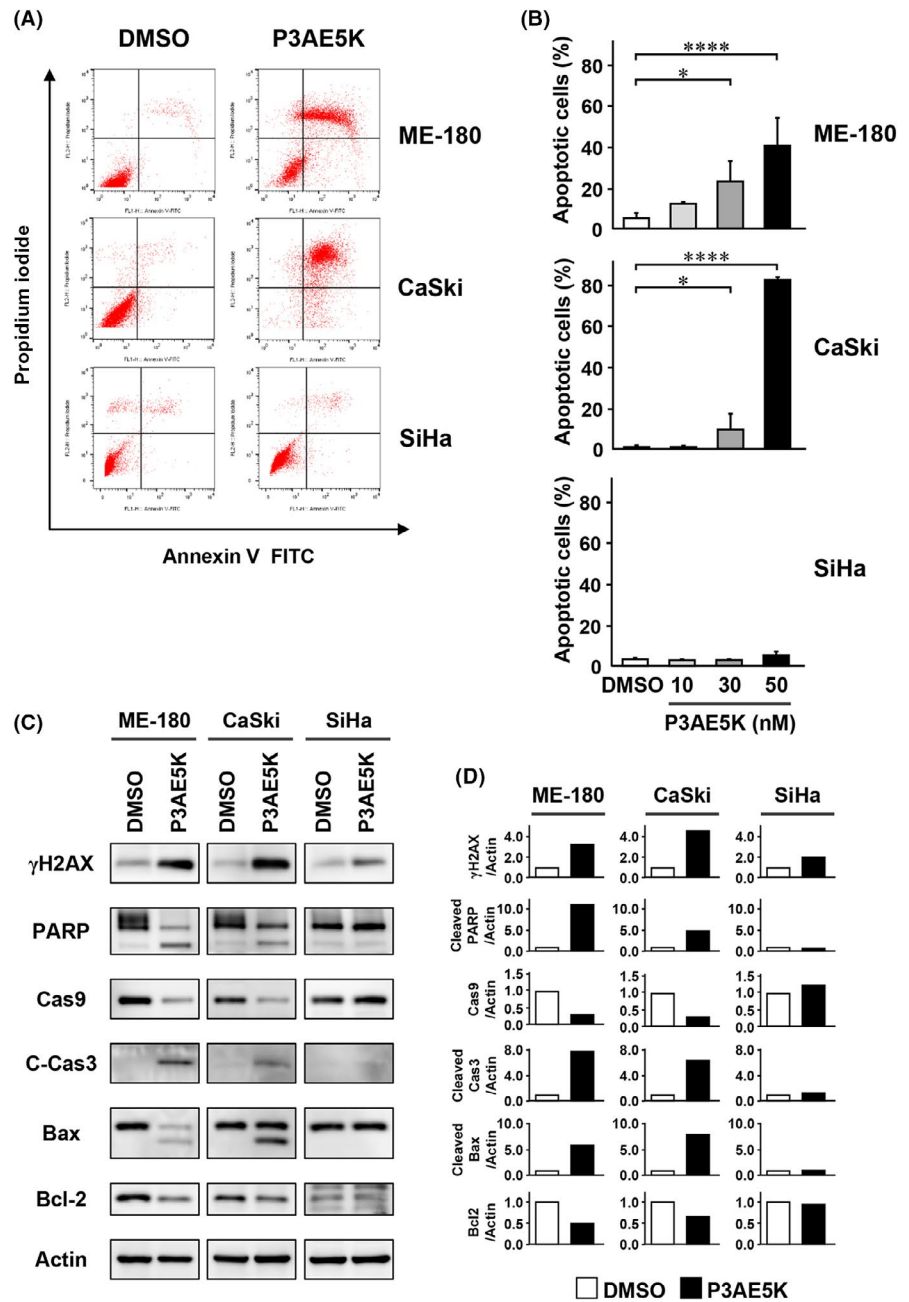
3.5 | P3AE5K reduced tumor growth in a cervical cancer xenograft mouse model

We next evaluated the antitumor efficacy of P3AE5K in cervical cancer cell xenograft models derived from CaSki cells. P3AE5K was intraperitoneally administered to CaSki cell-derived tumor-bearing mice at 3 mg/kg/wk for 4 wk (Figure 5). Tumor growth in the P3AE5K-treated group was significantly delayed compared with vehicle-treated mice ($P < .05$). At the end of treatment, tissue samples were collected from tumor, lung, liver and kidney and subjected to histological examination. H&E staining of the tumor tissues demonstrated that cell morphology was not uniform and cell shrinkage and chromatin condensation were observed in the P3AE5K-treated group (Figure 5C). Immunohistochemistry using anti-p110 α (*PIK3CA*) antibody demonstrated the reduced level of p110 α expression and Akt phosphorylation in the tumor tissues after P3AE5K treatment. The P3AE5K-treated group showed no decrease in body weight during the study (Figure S4A). H&E staining exhibited no obvious histopathological change in any organ tissues after P3AE5K treatment (Figure S4B), indicating its low systemic toxicity.

4 | DISCUSSION

Different types of cancer often harbor activating mutations in the *PIK3CA* gene, and these mutations frequently confer oncogenic transformation and drug resistance.^{17,30} The product of the genetically altered *PIK3CA* gene is involved in upregulation of the PI3K signaling pathway, which blocks pro-apoptotic signals and mediates cellular survival, leading to *PIK3CA* being considered as an important molecular target for cancer therapy. However, resistance to PI3K inhibitors is often observed in *PIK3CA* mutant-driven cancers, preventing their clinical use.^{12,31} One of the common mutations of *PIK3CA* is E545K, which can lead to constitutive PI3K α activity. We here propose an alternative approach using P3AE5K, an alkylating PI polyamide, to target the constitutively activating mutation of *PIK3CA* gene in cervical cancer cells. Our results suggested that P3AE5K can suppress mutant *PIK3CA* expression as a direct consequence of the PI polyamide covalently alkylating its DNA target site,³² which is a distinct mode of action from protein kinase inhibitors. P3AE5K exhibited lower IC₅₀ values in cervical cancer cell lines with E545K mutation of the *PIK3CA* gene compared with PI3K inhibitors. One possible explanation for the strong cytotoxicity of P3AE5K is that the reduced survival signal, due to the suppressed expression of mutant *PIK3CA*, leads to activation of pro-apoptotic signals. Additionally, silencing of *PIK3CA* may elevate the level of DNA damage in cells. PI3K inhibition has been reported to sensitize cancer cells with *PIK3CA* mutations to chemotherapeutic agents and radiotherapy.^{17,33} The synergistic effects of PI3K inhibitors and conventional cancer treatments were accompanied with suppressed downstream signals of PI3K pathways, which may result in impaired DNA damage repair.¹⁷ The alkylating PI polyamide was designed for 9 bases in the DNA duplex, including the mutation site of *PIK3CA* gene. Although it may also alkylate other genomic regions with the same binding motif, this is much less frequent compared with conventional alkylating agents

FIGURE 4 Apoptosis induced by P3AE5K treatment in cervical cancer cells. **A**, ME-180, CaSki and SiHa cells were treated with DMSO or 50 nmol/L of P3AE5K for 48 h. The percentage of apoptotic cells was quantified by Annexin V staining and flow cytometry. **B**, Comparison of percentages of apoptosis in cervical cancer cell lines treated with different concentrations of P3AE5K for 48 h. *P*-values were calculated from 3 independent experiments using one-way ANOVA followed by Holm-Sidak multiple comparison test (**P* < .05, *****P* < .0001). **C**, Cervical cancer cells were treated with P3AE5K (10 nmol/L) for 48 h. Immunoblotting for apoptotic and DNA damage markers was performed using antibodies against phospho-H2AX (γ H2AX), PARP, caspase 9 (Cas9), cleaved caspase 3 (C-Cas3), Bax and Bcl-2. Anti-actin antibody was used as an internal control. **D**, Densitometric quantification of western blot bands. The expression of each protein was normalized to actin and fold change relative to DMSO was calculated. Data are the average of 2 independent experiments



such as cyclophosphamide, cisplatin and so on. We speculated that P3AE5K may exert strong cytotoxicity against *PIK3CA* mutant cells because it suppresses *PIK3CA* expression and induces DNA damage as one agent.

ME-180 cells were more susceptible to P3AE5K and underwent apoptosis after low dose P3AE5K treatment compared with CaSki cells. Western blot analysis demonstrated that CaSki cells displayed relatively less apoptotic signals even though they received comparable DNA damage by P3AE5K to ME-180 cells. One possible cause of this difference could be some resistant mechanisms of P3AE5K in CaSki cells. Transcriptional downregulation of *PIK3CA* in ME-180 cells after P3AE5K treatment was more significant than that in CaSki cells. P3AE5K access to the *PIK3CA* mutation sequence may differ between ME-180 and CaSki cells. Anti-apoptotic Bcl-2 reduction

was also different between these cells, which might define their susceptibility to P3AE5K and/or apoptosis.

Pyrrole-imidazole polyamides allow for sequence-selective alkylation at a target site in the DNA duplex^{21,27,34} and SPR results also confirmed P3AE5K's selective affinity for the E545K-mutated *PIK3CA* sequence. This mode of sequence-specific alkylation by P3AE5K is likely to lead to preferential inhibition of E545K *PIK3CA* expression in cancer cells, although inhibition of the wild-type variant is unlikely. In addition to specific binding to the target DNA sequence, another important characteristic of PI polyamides is its low toxicity to normal cells and tissues.³⁵⁻³⁷ In the present study, intraperitoneal administration of P3AE5K once a week was tolerable to mice and exhibited antitumor activity. To further assess the effectiveness of P3AE5K as a therapeutic

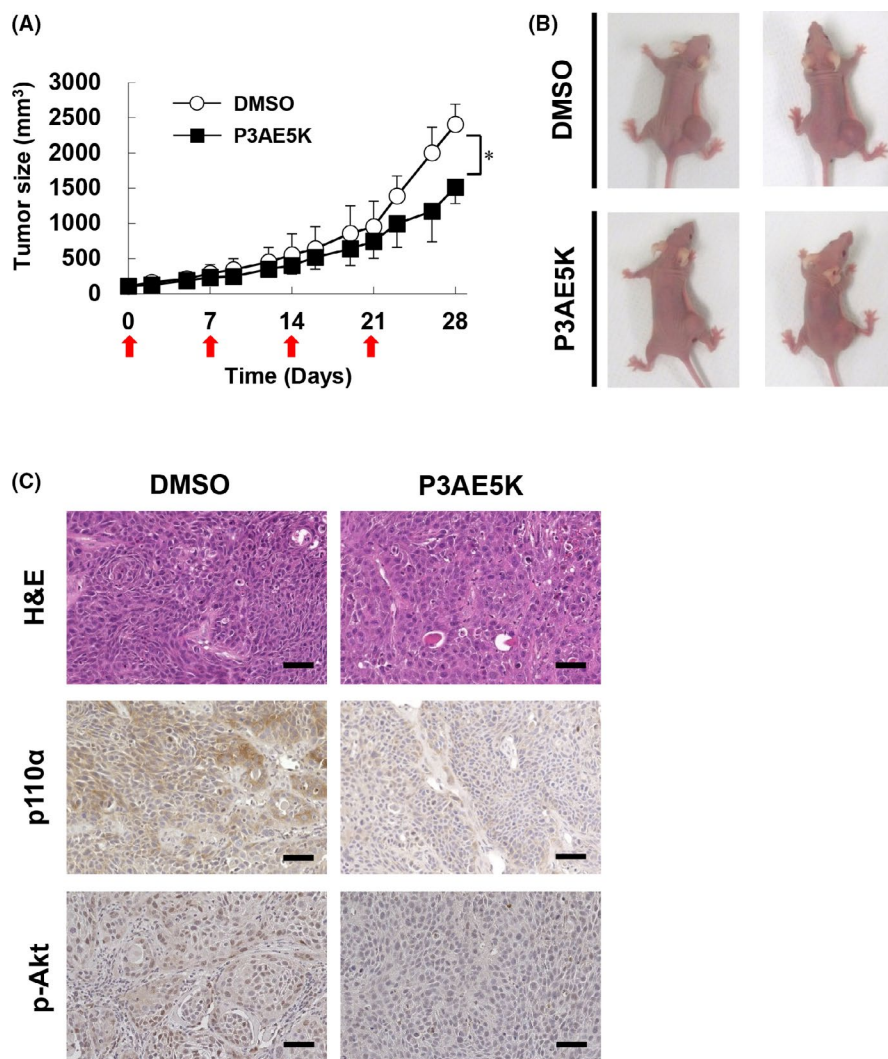


FIGURE 5 P3AE5K efficacy in a xenograft model. BALB/c nude mice bearing CaSki cell-derived xenografts were intraperitoneally injected with DMSO or 3 mg/kg of P3AE5K ($n = 6/\text{group}$) once a week for 4 wk (A). Data are represented as mean \pm SD and the difference in tumor volume between the 2 groups was evaluated using repeated measures ANOVA followed by Bonferroni post test ($*P < .05$). B, Representative images of mice in the indicated treatment groups at 28 d. C, Representative photographs from H&E staining and immunostaining using anti-p110 α and anti-phospho-Akt (p-Akt) antibodies of the sections from tumor tissues. Scale bars, 50 μ m

lead compound, we are currently evaluating the incorporation of our recently developed next-generation sequencing-based workflow³⁸ to detect the genome-wide effect of P3AE5K's genomic binding and to determine the overall pharmacological impact of P3AE5K.

In conclusion, the approach undertaken here with P3AE5K allowed the hotspot E545K mutation of the *PIK3CA* gene to be directly targeted and silenced at the genome level, resulting in downregulation of *PIK3CA* gene expression and retardation of tumor growth in mice. These results suggested that P3AE5K should be an attractive drug candidate for targeting E545K-mutated *PIK3CA* gene in cervical cancers, which are still a major "mother killer" in countries where HPV vaccination is not available.

ACKNOWLEDGMENTS

We thank Tomoko Koga, Rie Igarashi and Takako Akahira for providing technical support for this project. We thank the Edanz Group (www.edanzediting.com/ac) for editing a draft of this manuscript. This work was supported in part by the Princess Takamatsu Cancer Research Fund to HN, JSPS KAKENHI [Grant Number JP26290060, JP17H03602 and JP16H01579] to HN, MEXT KAKENHI [Grant

Number JP25830092] to AT and Takeda Science Foundation to AT. We thank the Otsuka Toshimi Scholarship Foundation for providing financial assistance to SK.

DISCLOSURE

We have no conflicts of interest to disclose.

ORCID

HiroYuki Yoda  <https://orcid.org/0000-0002-5528-8940>

Jason Lin  <https://orcid.org/0000-0002-8086-3185>

Atsushi Takatori  <https://orcid.org/0000-0002-2184-6721>

Hiroki Nagase  <https://orcid.org/0000-0002-3992-5399>

REFERENCES

1. Ferlay J, Soerjomataram I, Dikshit R, et al. Cancer incidence and mortality worldwide: sources, methods and major patterns in GLOBOCAN 2012. *Int J Cancer*. 2015;136:E359-E386.
2. Henken FE, Banerjee NS, Snijders PJ, et al. PIK3CA-mediated PI3-kinase signalling is essential for HPV-induced transformation in vitro. *Mol Cancer*. 2011;10:71.
3. Monk BJ, Sill MW, McMeekin DS, et al. Phase III trial of four cisplatin-containing doublet combinations in stage IVB, recurrent,

- or persistent cervical carcinoma: a Gynecologic Oncology Group study. *J Clin Oncol*. 2009;27:4649-4655.
4. Hou MM, Liu X, Wheler J, et al. Targeted PI3K/AKT/mTOR therapy for metastatic carcinomas of the cervix: a phase I clinical experience. *Oncotarget*. 2014;5:11168-11179.
 5. Bertelsen BI, Steine SJ, Sandvei R, et al. Molecular analysis of the PI3K-AKT pathway in uterine cervical neoplasia: frequent PIK3CA amplification and AKT phosphorylation. *Int J Cancer*. 2006;118:1877-1883.
 6. Kandoth C, McLellan MD, Vandin F, et al. Mutational landscape and significance across 12 major cancer types. *Nature*. 2013;502:333-339.
 7. Mjos S, Werner HMJ, Birkeland E, et al. PIK3CA exon9 mutations associate with reduced survival, and are highly concordant between matching primary tumors and metastases in endometrial cancer. *Sci Rep*. 2017;7:10240.
 8. Zhang L, Wu J, Ling MT, et al. The role of the PI3K/Akt/mTOR signalling pathway in human cancers induced by infection with human papillomaviruses. *Mol Cancer*. 2015;14:87.
 9. Wright AA, Howitt BE, Myers AP, et al. Oncogenic mutations in cervical cancer: genomic differences between adenocarcinomas and squamous cell carcinomas of the cervix. *Cancer*. 2013;119:3776-3783.
 10. Chen IC, Hsiao LP, Huang IW, et al. Phosphatidylinositol-3 Kinase Inhibitors, Buparlisib and Alpelisib, Sensitize Estrogen Receptor-positive Breast Cancer Cells to Tamoxifen. *Sci Rep*. 2017;7:9842.
 11. Engelman JA. Targeting PI3K signalling in cancer: opportunities, challenges and limitations. *Nat Rev Cancer*. 2009;9:550-562.
 12. Rodon J, Dienstmann R, Serra V, et al. Development of PI3K inhibitors: lessons learned from early clinical trials. *Nat Rev Clin Oncol*. 2013;10:143-153.
 13. Chandralapaty S, Sawai A, Scaltriti M, et al. AKT inhibition relieves feedback suppression of receptor tyrosine kinase expression and activity. *Cancer Cell*. 2011;19:58-71.
 14. Rozengurt E, Soares HP, Sinnet-Smith J. Suppression of feedback loops mediated by PI3K/mTOR induces multiple overactivation of compensatory pathways: an unintended consequence leading to drug resistance. *Mol Cancer Ther*. 2014;13:2477-2488.
 15. Serra V, Scaltriti M, Prudkin L, et al. PI3K inhibition results in enhanced HER signaling and acquired ERK dependency in HER2-overexpressing breast cancer. *Oncogene*. 2011;30:2547-2557.
 16. Lee CM, Fuhrman CB, Planelles V, et al. Phosphatidylinositol 3-kinase inhibition by LY294002 radiosensitizes human cervical cancer cell lines. *Clin Cancer Res*. 2006;12:250-256.
 17. Arjumand W, Merry CD, Wang C, et al. Phosphatidylinositol-3 kinase (PIK3CA) E545K mutation confers cisplatin resistance and a migratory phenotype in cervical cancer cells. *Oncotarget*. 2016;7:82424-82439.
 18. Dervan PB, Edelson BS. Recognition of the DNA minor groove by pyrrole-imidazole polyamides. *Curr Opin Struct Biol*. 2003;13:284-299.
 19. Wurtz NR, Dervan PB. Sequence specific alkylation of DNA by hairpin pyrrole-imidazole polyamide conjugates. *Chem Biol*. 2000;7:153-161.
 20. Chenoweth DM, Dervan PB. Allosteric modulation of DNA by small molecules. *Proc Natl Acad Sci U S A*. 2009;106:13175-13179.
 21. Hiraoka K, Inoue T, Taylor RD, et al. Inhibition of KRAS codon 12 mutants using a novel DNA-alkylating pyrrole-imidazole polyamide conjugate. *Nat Commun*. 2015;6:6706.
 22. Kurmis AA, Yang F, Welch TR, et al. A Pyrrole-imidazole polyamide is active against enzalutamide-resistant prostate cancer. *Cancer Res*. 2017;77:2207-2212.
 23. Syed J, Pandian GN, Sato S, et al. Targeted suppression of EVI1 oncogene expression by sequence-specific pyrrole-imidazole polyamide. *Chem Biol*. 2014;21:1370-1380.
 24. Wang X, Nagase H, Watanabe T, et al. Inhibition of MMP-9 transcription and suppression of tumor metastasis by pyrrole-imidazole polyamide. *Cancer Sci*. 2010;101:759-766.
 25. Bando T, Sugiyama H. Synthesis and biological properties of sequence-specific DNA-alkylating pyrrole-imidazole polyamides. *Acc Chem Res*. 2006;39:935-944.
 26. Matsuda H, Fukuda N, Ueno T, et al. Development of gene silencing pyrrole-imidazole polyamide targeting the TGF-beta1 promoter for treatment of progressive renal diseases. *J Am Soc Nephrol*. 2006;17:422-432.
 27. Taylor RD, Asamitsu S, Takenaka T, et al. Sequence-specific DNA alkylation targeting for Kras codon 13 mutation by pyrrole-imidazole polyamide seco-CBI conjugates. *Chem Eur J*. 2014;20:1310-1317.
 28. Lajiness JP, Boger DL. Asymmetric synthesis of 1,2,9,9a-tetrahydrocyclopropa[c]benzo[e]indol-4-one (CBI). *J Org Chem*. 2011;76:583-587.
 29. Valko K, Du CM, Bevan CD, et al. Rapid-gradient HPLC method for measuring drug interactions with immobilized artificial membrane: comparison with other lipophilicity measures. *J Pharm Sci*. 2000;89:1085-1096.
 30. Zhao JJ, Gjoerup OV, Subramanian RR, et al. Human mammary epithelial cell transformation through the activation of phosphatidylinositol 3-kinase. *Cancer Cell*. 2003;3:483-495.
 31. Mayer IA, Abramson VG, Formisano L, et al. A Phase Ib study of alpelisib (BYL719), a PI3Kalpha-specific inhibitor, with letrozole in ER+/HER2- metastatic breast cancer. *Clin Cancer Res*. 2017;23:26-34.
 32. Shinohara K, Sasaki S, Minoshima M, et al. Alkylation of template strand of coding region causes effective gene silencing. *Nucleic Acids Res*. 2006;34:1189-1195.
 33. Zumsteg ZS, Morse N, Krigsfeld G, et al. Taselisib (GDC-0032), a Potent beta-sparing small molecule inhibitor of PI3K, radiosensitizes head and neck squamous carcinomas containing activating PIK3CA alterations. *Clin Cancer Res*. 2016;22:2009-2019.
 34. Bando T, Sasaki S, Minoshima M, et al. Efficient DNA alkylation by a pyrrole-imidazole CBI conjugate with an indole linker: sequence-specific alkylation with nine-base-pair recognition. *Bioconjug Chem*. 2006;17:715-720.
 35. Liu K, Fang L, Sun H, et al. Targeting polo-like kinase 1 by a novel pyrrole-imidazole polyamide-hoechst conjugate suppresses tumor growth in vivo. *Mol Cancer Ther*. 2018;17:988-1002.
 36. Mishra R, Watanabe T, Kimura MT, et al. Identification of a novel E-box binding pyrrole-imidazole polyamide inhibiting MYC-driven cell proliferation. *Cancer Sci*. 2015;106:421-429.
 37. Yang F, Nickols NG, Li BC, et al. Animal toxicity of hairpin pyrrole-imidazole polyamides varies with the turn unit. *J Med Chem*. 2013;56:7449-7457.
 38. Lin J, Hiraoka K, Watanabe T, et al. Identification of binding targets of a pyrrole-imidazole polyamide KR12 in the LS180 colorectal cancer genome. *PLoS One*. 2016;11:e0165581.

SUPPORTING INFORMATION

Additional supporting information may be found online in the Supporting Information section.

How to cite this article: Krishnamurthy S, Yoda H, Hiraoka K, et al. Targeting the mutant *PIK3CA* gene by DNA-alkylating pyrrole-imidazole polyamide in cervical cancer. *Cancer Sci*. 2021;112:1141-1149. <https://doi.org/10.1111/cas.14785>